Initial Findings from Continuous Monitoring of Oil and Gas Operations

William Daniels*[1,2], James Crompton[3], Dorit Hammerling[1], and Morgan Bazilian[2]

[1]Department of Applied Mathematics and Statistics, Colorado School of Mines, Golden CO
[2]Payne Institute for Public Policy, Colorado School of Mines, Golden CO
[3]Department of Petroleum Engineering, Colorado School of Mines, Golden CO

Abstract

Through the wide deployment of air quality monitoring technology, we can better address greenhouse gas emissions from the oil and gas industry. There is considerable public pressure, industry engagement, and government regulation surrounding the push for more sophisticated and transparent monitoring. While much focus has been given to the technological development of monitoring devices and the use of airplane and LDAR resources, less focus has been given to the data acquisition, management, and analysis from these monitoring technologies. This paper presents an exploratory analysis of continuous monitoring data from two oil and gas sites in Colorado. Specifically, we highlight initial results from ongoing research into three areas: trend isolation for better use of continuous monitoring data in predictive models, anonymized metrics for presentation in a public facing dashboard, and source localization using meteorological data. The paper demonstrates some of the capabilities (as well as the challenges) of using continuous monitoring data in addressing greenhouse gas emissions and provides areas for further research.

Keywords: continuous monitoring, oil and gas, methane, volatile organic compounds, particular matter, time series analysis

*wdaniels@mines.edu

1 Introduction

The growing concern over greenhouse gas (GHG) emissions is spurring change in the oil and gas (O&G) industry. Regulators are focusing on the environmental effects and the health and safety of oilfield operations [1–3]. NGOs are concentrating on ways to better understand the impact of methane and other GHGs on climate change [4]. ESG investors are requiring the energy industry to demonstrate their commitment to carbon-neutral plans and strategies [1].

Many larger operators are working to rebalance their portfolios toward low-carbon projects as they seek to become the broad-based energy companies of the future [5–7]. At the same time, the industry is looking for ways to produce more oil and gas (and increasingly power) to respond to forecasted energy demand, while also being carbon conscious. These companies will need to operate a range of assets, develop novel technologies, and enter new markets. The need for better monitoring is becoming apparent if natural gas is to fill its role as a bridge fuel for this upcoming energy transition.

Emissions monitoring can be performed using an array of platforms: ground based "fenceline" sensors, drones and aircraft, and satellite. [8]. Satellite data has long been used as a means of monitoring column-averaged methane concentrations on a global scale, but suffers from a coarse spatial resolution [9–11]. Drones and aircraft provide a more targeted top-down emission estimate, and much work has been done to develop and perform monitoring campaigns [12–19]. Finally, LDAR and in situ monitoring can be used to estimate emissions from specific pieces of equiptment at various timescales but is hard to deploy across an entire basin [20–28]. Each approach in this "digital canopy" will have its pros and cons, and a hybrid of solutions will likely be needed [29]. Project Canary (a certified B Corporation) seeks to address this need for better monitoring, specifically the ground-based continuous monitoring layer of the digital canopy, by providing a continuous system for detecting volatile organic compounds (VOCs) and methane [30].

When placed around an O&G site, these units provide operators with real time data and emission alerts. By placing units on multiple sites, operators can monitor their basin wide impact. With the cooperation of both Project Canary and their industry partners, continuous monitoring data from dozens of O&G sites across Colorado are being sent to the Payne Institute for Public Policy in real time. Therefore, the Payne Institute (a research institute affiliated with the Colorado School of Mines) can serve as a neutral third party to both hold these data and interface with regulators or government agencies in the future. In addition to acting as a neutral repository, the Payne Institute has undertaken an exploratory analysis of the Canary data.

This paper seeks to demonstrate a selection of features from these continuous monitoring data and highlight future areas of study. Note that while this paper focuses on the Project Canary data, these methods can be applied to any system that provides near continuous observations of atmospheric pollutants or meteorological fields. Also note that a description of the data repository, data transfer, and data security measures that the Payne Institute has developed is planned for a separate paper.

2 Project Canary Continuous Monitoring System

Project Canary has developed a solar powered air quality and meteorological monitoring system (Figure 1). Measurements are made every second, and minute averages are sent to the Project Canary cloud platform using cellular communication.

The units are capable of measuring concentrations of the following air quality indicators:

- Volatile organic compounds (VOCs)
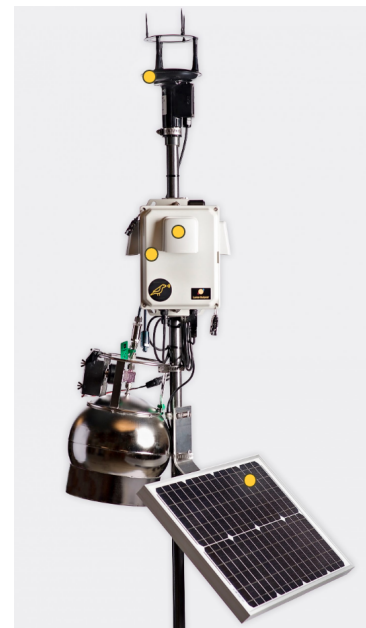- Particulate matter with diameter of 10 μm and smaller (PM_10)

Figure 1: Canary unit (Model S).

- Particulate matter with diameter of 2.5 μm and smaller (PM_2.5)
- Particulate matter with diameter of 1 μm and smaller (PM_1)
- Methane (CH_4)

However, not all units currently have the required sensor to measure methane. In addition, the units measure the following meteorological fields:

- Wind speed and direction
- Air pressure
- Temperature
- Humidity

Typically, three to four units are placed on the fenceline of each O&G site (around 100 feet from the O&G equipment). The units are placed so that they surround the facility, therefore maximizing coverage and making leak detection more likely. In this paper, we focus our analysis on VOC and PM measurements, as the methane sensors are not yet widely distributed to the Canary units in Colorado.

3   Demonstration of Continuous Monitoring Data

In this section, we will show two data samples with the intention of highlighting the "raw" data produced by these types of continuous monitoring systems as well as the challenges in their interpretation. Both samples are taken from an O&G facility in Colorado referred to as "Site A" to protect operator anonymity.

Figure 2 shows the geometry of Site A, with locations of the Canary units marked with X's. The first sample will highlight a "standard" day, or a day where no anomalous VOC or PM concentrations were recorded. The second sample will highlight an abnormal spike in both VOC and PM.

It is important to note that at this point in our analysis, we do not attempt to attribute an abnormal spike in VOCs or PM to any potential source. The VOC and PM events highlighted in this paper could have been caused by a planned operational event, a fugitive emission, or a source completely unaffiliated with the O&G facility. Attributing a particular spike in the data to a specific aspect of O&G operations (or otherwise) is an ongoing research topic, and our initial progress is discussed further in Section 4.

Figure 2: Geometry of Site A. Locations of the four Canary units are marked with X's. The northwest unit is the only unit on site that measures wind.

3.1   Typical Day

One of the benefits of continuous monitoring is the rapid detection of emissions. However, before highlighting an abnormal VOC and PM_2.5 event, we believe that there is value in first understanding the signals from a "typical" day in which no abnormal events occur. One such day is shown in Figure 3.

The bottom two plots show the PM_2.5 and VOC signal over the course of the day (August 1, 2020). The data we have chosen to present starts and ends at midnight, and the four signals are from the four Canary units on the site. The day has been divided into four sections, and the wind speed and direction have been aggregated over each section and are
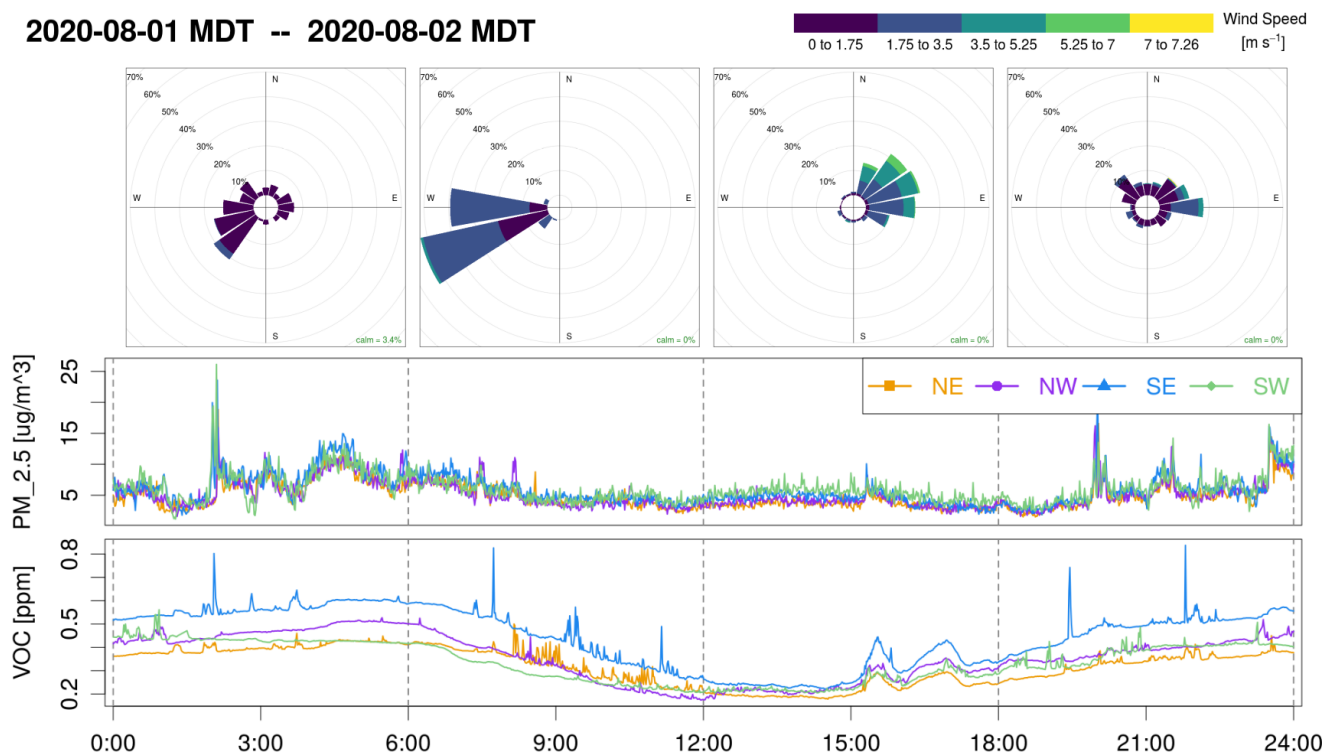
Figure 3: Canary data on a typical day. From top to bottom: 6 hour wind aggregations over the course of the day, PM_2.5 signal from each Canary unit on site, and VOC signal from each Canary unit on site.

shown above the two signals as rose plots. The angle of each wedge in the rose plots indicates the direction from which the wind originates, and the length of the wedge indicates the relative amount of time that the wind came from that direction. The color of the wedges corresponds to the speed of the wind, with the sizes of each color representing the relative time at each speed.

The VOC signal fluctuates throughout the day, but never by more than about 0.3 ppm (i.e. 9:00 to 12:00 and 15:00 to 18:00). Fluctuations of this magnitude are quite common in the VOC signal, and could be caused by any number of natural or anthropogenic sources. There also appears to be a diurnal cycle present in the VOC signal, with higher concentrations at night and lower concentrations during the day. This makes sense, as most VOCs react with sunlight to form other compounds. We have done some initial work in generalizing this diurnal cycle as well as a longer term trend in the VOC signal, which we discuss further in Section 4. Additionally, we can see that the southeast unit reads slightly higher VOC concentrations than the other three, primarily at night. Again, this could be due to a number of natural or anthropogenic sources. For instance, the O&G equipment in the southeast corner might be a consistent source of low volume VOCs. Alternatively, the surrounding farmland might produce more VOCs near the southeast sensor than the other three. This feature could also be due to the amount of sunlight each unit receives.

Unlike the VOC signal, the PM signal does does display a clear diurnal cycle. This is likely because PM concentrations are not closely tied to sunlight, as is the case with VOCs. The PM signal is much noisier than the VOC signal, likely due to sensitivity differences between the two sensors. The wind data reveals that there was no predominant wind direction over the course of the day. Since there were no major VOC or PM events during this day, there is not much to compare the wind data against. We have begun initial work into comparing wind direction to VOC events, which is discussed further in Section 4. Note that the wind data comes from only one unit per site, in this case the northwest unit.
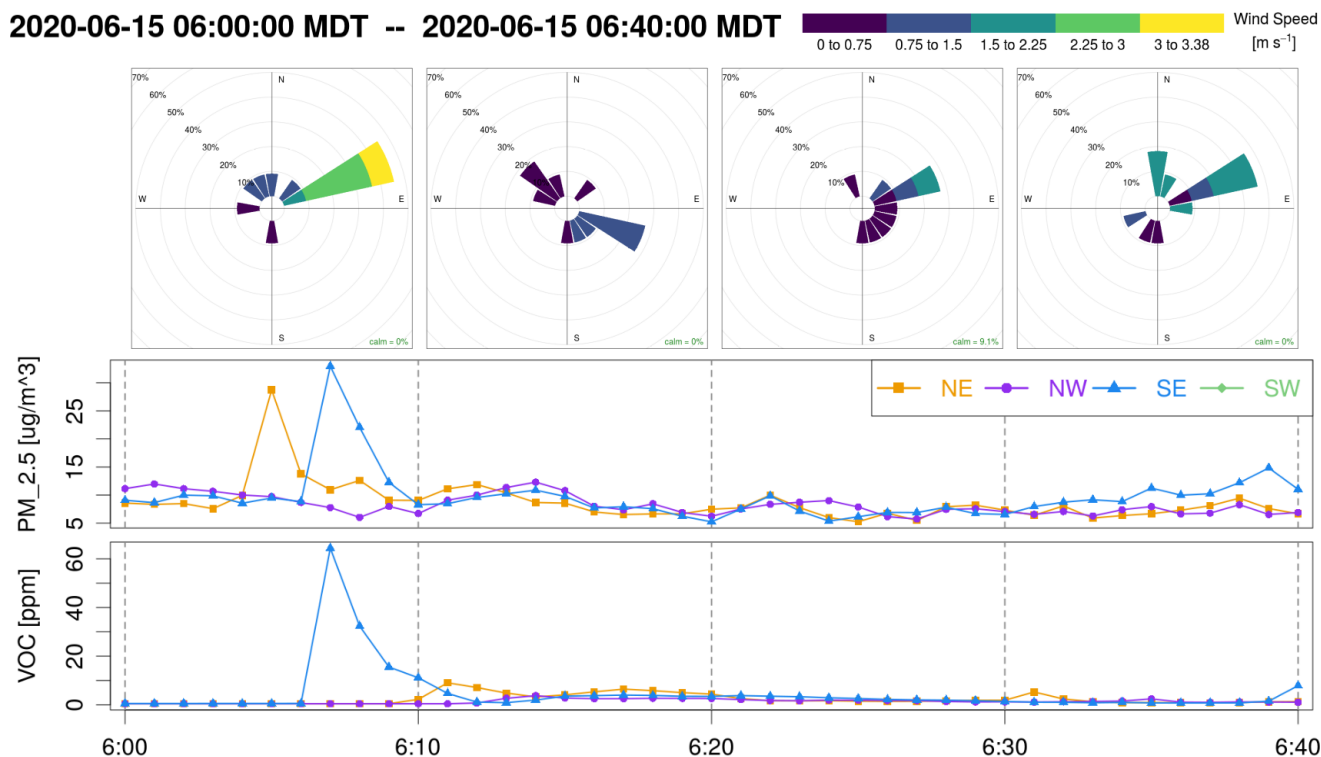
Figure 4: Canary data during an abnormal VOC and PM event. From top to bottom: 10 minute wind aggregations over the course of the event, PM_2.5 signal from each Canary unit on site, and VOC signal from each Canary unit on site.

3.2 Abnormal VOC and PM Event

We now highlight an abnormal spike in both VOCs and PM. This data sample spans only 40 minutes to highlight the details of the event (Figure 4).

At 6:07am there is a spike in both PM and VOC. While the PM spike is similar in magnitude to some of the spikes shown in Figure 3, the VOC spike is much more significant. The median VOC concentration from this site is on the order of 0.5 ppm (discussed more in Section 4). This event is a clear departure from the standard concentrations. Again, at this point in our analysis, we make no conclusions as to the source of this event. Our goal is rather to present the data as is, highlight notable features, and discuss the challenges in drawing causal conclusions.

We can see that during the 10 minute section in which the spike occurs, the wind is blowing at moderate intensity out of the northeast. Therefore, the spike could be attributed to the farmland to the northeast of the O&G facility. Alternatively, it could be attributed to a fugitive (or operational) emission strong enough to reach the northeast and southeast sensors, regardless of wind direction. Additionally, the spike might have resulted from a vehicle driving past both the northeast and southeast sensors. Without more data, we are hesitant to make any claims beyond simply stating that an event occurred. Note that we are currently working on an algorithm to not only identify when a spike occurs, but to attribute the spike to a specific location on the site and include a measure of uncertainty with this attribution (see Section 4).

4 Exploratory Analysis

We now present initial results from three research areas we are actively pursuing. We hope that this section demonstrates some of the capabilities of continuous monitoring data in addressing green house gas emissions from O&G sites.
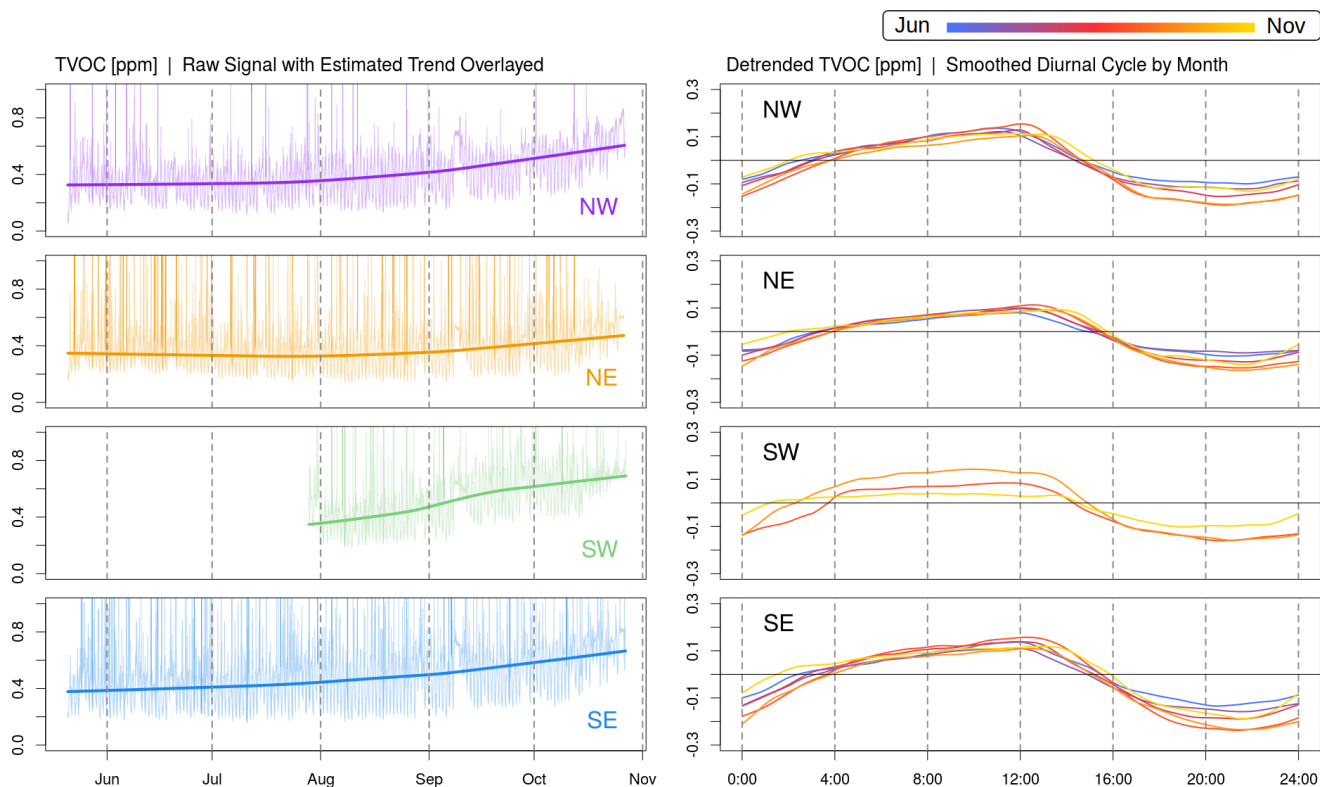
Figure 5: **Left**: raw VOC data from the four Canary units on Site A and our estimate of the long-term VOC trend. **Right**: our estimates of the diurnal cycle in the VOC signal for each Canary unit, broken up by month.

4.1 Trend Isolation for Better use in Predictive Models

An interesting application of continuous monitoring data is its use in predictive models. In particular, there is potential to predict future VOC (or methane) events using additional operation data, such as tank or separator pressures. This would allow operators to potentially intervene before an emission event occurs.

However, when using time series data in predictive models, it is advantageous to isolate and remove both long-term trends and cyclical patterns (this is related to the idea of *stationarity*). In this way, predictive models are better able to detect the anomalous events of interest (i.e. fugitive emissions) rather than the natural trends in the data, like the diurnal cycle in VOC concentrations caused by sunlight.

We have attempted to isolate both a longer term trend and a daily cycle in the Canary VOC signal (Figure 5). The left-hand column shows the raw VOC signal from the four units on Site A. Note that these plots span significantly more time than Figures 3 and 4, hence the apparent increase in VOC spikes. Plotted over the raw signal is a smoothed curve produced via LOWESS (a non-parametric method that involves locally weighted polynomial regression). Until we obtain multiple years of data, this smoothed curve will serve as our estimate of the long-term trend in the VOC signal. It is quite likely that this curve is actually capturing part of a yearly cycle, where VOC concentrations are higher in winter and lower in summer (recall that sunlight destroys VOCs). However, with less than a year of data, we are unable to better estimate this yearly cycle. To produce a detrended VOC signal, we simply subtract these trends from the VOC data of the respective Canary units.

The right-hand column of Figure 5 shows our estimate of the previously mentioned diurnal cycle in VOC concentrations. Each plot corresponds to one of the Canary units on Site A, and each curve represents our estimate for a given month. The months proceed sequentially from June (blue) to November (gold). These curves were produced using the detrended data and are therefore centered around zero. Our procedure for estimating this cycle is as follows: 1) detrend the VOC signals, 2) using one month of detrended VOC data at a time, compute the median VOC value at each minute, 3) smooth the curves produced by these median values.
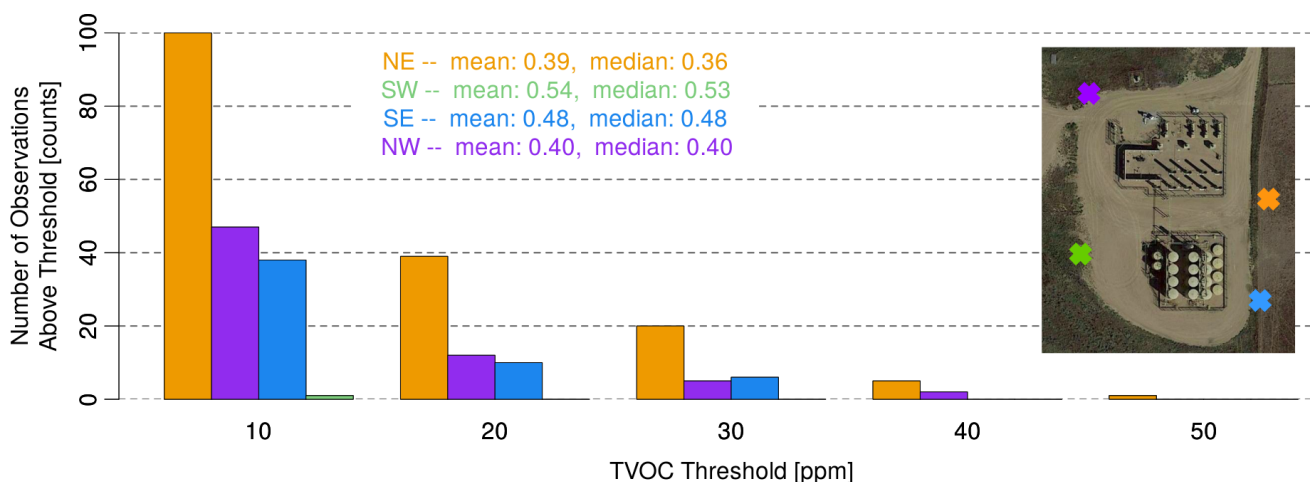
6

Figure 6: Number of VOC observations above a selection of thresholds. This is one example of a metric can that be displayed in an O&G monitoring dashboard.

As expected, the VOC concentrations are higher at night and lower during the day, as sunlight reacts with VOCs to create other compounds. A close examination of the individual curves will reveal subtle differences from month to month, but these details are not discussed here. To remove this daily cycle from the VOC data, we again simply subtract the curve for each month from the already detrended signal.

The result of this detrending effort is twofold. First, we are left with detrended, deseasonalized data that is better suited for use in predictive models. This procedure can be easily applied to methane data once the methane sensors are more widely distributed across the Colorado units. Second, the detrending process results in an interesting byproduct: estimates for both the long-term trend and daily cycle in VOCs. Other detrending methods (i.e. differencing) do not produce such estimates, which have many potential scientific uses.

4.2 VOC Thresholds for Presentation of Basin-Wide Metrics

Another application of continuous monitoring data is a dashboard of metrics available to the O&G industry, regulators, or the public. This dashboard could provide an avenue for O&G companies that are working hard to reduce their emissions to showcase their efforts. It could also be used by government regulators to provide incentives to compliant companies.

Any number of metrics could be presented in this dashboard, and here we showcase an example. After observing an abnormal VOC event (such as the one in Figure 4), one might be interested in the number of these events over a given period of time. Figure 6 attempts to address this. On the horizontal axis we have created five VOC thresholds. Note that these thresholds are much larger than the standard VOC readings. For a relative sense of magnitude, the mean and median VOC value from each unit on Site A is listed above the bar plots. For each threshold, we simply count the number of VOC observations from each unit that are above this value. The vertical axis can therefore be interpreted as either the number of observations above each threshold, or alternatively as the cumulative time above each threshold (since each observation is a minute average).

Note that this chart does not indicate the number of *separate* events that occurred above each threshold, but rather the total number of observations above each threshold. Therefore, the counts presented here could be from a single large event that spent considerable time above the threshold or from multiple smaller events that each spent very little time above the threshold. Being able to classify VOC spikes as separate events would require more sophisticated algorithms. Also note that these counts do not estimate source volumes, but rather examine the ambient VOC concentrations at the units.

We can see that the northeast sensor, while reading the lowest VOC concentrations on average, consistently observes more VOC spikes than the other three units across our five thresholds. Again, this disparity in VOC

spikes could be from a variety of sources. For instance, the northeast portion of the O&G facility might be a more consistent emitter of VOCs. This unit might also be positioned closer to where transport vehicles typically operate. Another possibility is that these spikes are a result of some source not affiliated with the O&G facility. Without additional data or information, it is hard to attribute these spikes to any particular source.

We hope that Figure 6 will serve as an example of the type of metrics that can be presented in a data dashboard. Future work involving such a dashboard is discussed further in Section 5.

4.3   Source Localization using Wind Direction

A third application of continuous monitoring data is to inform operators not only when an abnormal VOC event is occurring, but to provide an estimate of where the potential source is located. This would help Leak Detection and Repair (LDAR) technicians more rapidly respond to potential emissions. Additionally, it could help discern O&G related emissions from emission sources external to the O&G facility.

The basis for this source localization algorithm is comparing wind direction to observed VOC spikes. In this section we present initial findings from this wind direction study. Future work on the leak detection algorithm will be discussed in Section 5.

As a test case, we will highlight a known leak event from a different O&G site in Colorado (Figure 7). This site will be referred to as "Site B" to protect operator anonymity. Site B has three Canary units and experienced a thief catch leak in early October that spanned two days before being addressed. The green rectangle in Figure 7 shows the location of the leaking thief hatches.

We will use 12 hours of data from this event to highlight our wind direction study. Since we already know the location of the emission source in this test case, we can highlight periods in which the wind is blowing from the source to each unit. Figure 8 shows the VOC signal from each Canary unit. Highlighted with vertical lines are the times in which the wind blew from the source to the unit. For instance, when considering the north unit, the times highlighted in purple indicate wind blowing from the southeast. When considering the west unit, the times highlighted in orange indicate wind blowing from the east-northeast. The times highlighted in red indicate strong wind speed.

Figure 7: Geometry of Site B. The green rectangle shows the location of four leaking thief hatches.

The north unit does not see any clear overlap between wind blowing from the source and observed VOC spikes. This is likely because the unit is so close to the emission source. We hypothesize that if the source is emitting VOCs, the north unit will pick it up, regardless of the wind direction. The west unit, on the other hand, sees a clear overlap between wind blowing from the source and observed VOC spikes. In fact, every notable VOC spike in this 12 hour time span is accompanied by wind blowing from the source to the unit. Finally, the south unit does not detect any large VOC spikes, making a comparison to the wind direction impossible.

We believe that the result of this wind direction study will lay the groundwork for an emission location algorithm, which is being actively pursued and is discussed further in Section 5. Considering just the wind direction study, however, we can see that the VOC signal from each unit is highly dependent on the position of the unit and the wind conditions. With further analysis, this can hopefully help inform sensor positioning in the future.
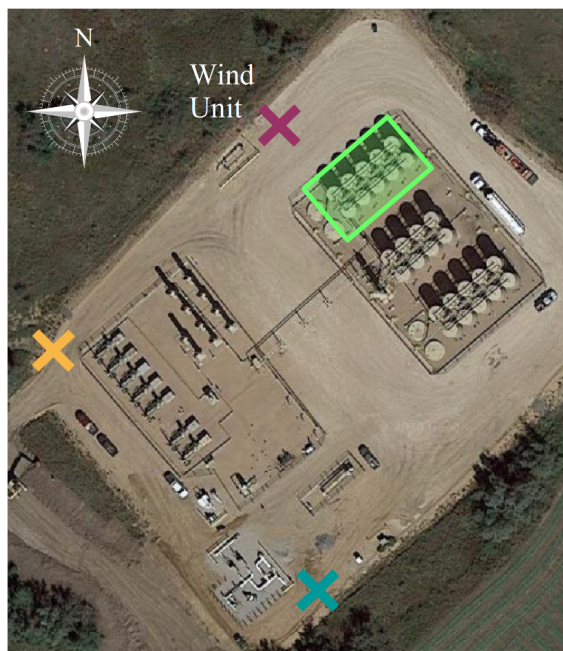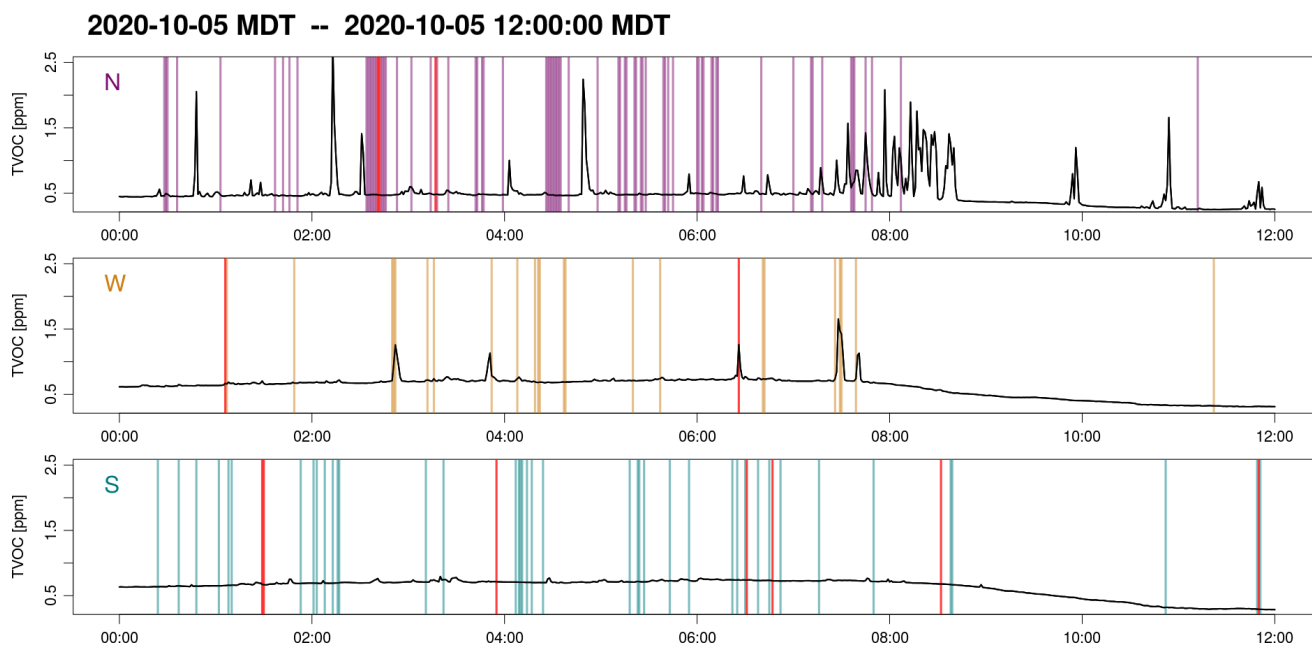
2020-10-05 MDT -- 2020-10-05 12:00:00 MDT

Figure 8: Site B Canary signals during a known leak event. Highlighted in color are times when the wind is blowing from the emission source to the unit. Red lines indicate periods of strong wind.

5 Conclusions and Future Directions

The purpose of this document is to present representative samples of O&G continuous monitoring data, highlight a selection of our exploratory analysis, and discuss future areas of research. In Section 3, we presented two data samples: a typical day and an anomalous VOC event. We hope that these samples are able to familiarize the reader with unprocessed continuous monitoring data. Some features to note in these samples are the relative levels of noise between PM and VOCs, the magnitude of the respective signals, and the use of wind data to further elucidate our picture of the O&G facility. In Section 4, we highlight three results from our exploratory analysis of these data. Notable results from this analysis include: detrended and de-seasonalized data prepped for predictive models, a sample metric that could be anonymized and presented in a public dashboard, and a framework that can potentially be used for emission source localization.

There is great potential for future research using continuous monitoring data. Listed here are a few direction that we are currently pursuing or are interested in pursuing.

- *Comparison of Canary and satellite data.* Satellite data has great potential for monitoring methane emissions from the O&G industry due to its global coverage. However, there are serious limitations of satellite data as well (namely its coarse spatial and temporal resolution). Continuous monitoring data provides a unique test environment in which the satellite data can be compared to site-level local monitoring. This has potential to inform what size emissions can be detected from space.

- *Dashboard of metrics.* As discussed throughout the text, we hope to create a dashboard of properly anonymized metrics to present to industry, regulators, or the general public. We hope to work closely with industry partners so that they are comfortable sharing abstractions or anonymizations of their data through a public facing dashboard. This has implications for both creating and enforcing data driven regulations, as well as highlighting companies who are ahead of the curve in their emission reduction efforts. Conversely, this could be used to point regulators to regions or O&G facilities that are non-compliant.

9

- *Leak localization algorithm.* Using the wind direction study discussed in Section 4.3 as a framework, we are exploring Monte Carlo methods for estimating source locations that are not known beforehand, like in the test case discussed earlier. This could help operators rapidly address unwanted emissions and discern when external air pollution sources are being picked up by continuous monitoring units.

- *Predictive models using operator SCADA data.* With additional data related to the O&G facility (such as tank pressures, separator pressures, tank temperatures, etc.) we could use the detrended data discussed in Section 4.1 to train predictive models. These models could be used to warn operators ahead of time if an emission event is likely based on certain facility conditions.

Appendix A   Methods

A.1   VOC Signal Decomposition

One way to better understand a signal (y_t) is to decompose it into trend (T_t), seasonal (D_t), and remainder (R_t) components. We have performed this technique on the Canary VOC data. We assume an additive decomposition, namely

$$y_t = T_t + D_t + R_t,$$

as the magnitude of the variability captured by D_t appears independent of time t. Note that this assumption is based on a relatively small amount of data and might require reconsideration as more data becomes available.

The seasonal component, D_t, captures periodic variability in y_t. We use this component to isolate the diurnal cycle present in the VOC data. The trend component, T_t, captures aperiodic variability of y_t that is not accounted for by D_t. We use this term to capture the increase in VOC concentrations on a monthly timescale. Note that this trend is likely part of a yearly cycle, with higher concentrations in winter and lower concentrations in summer. However, with data spanning less than a full period, we are unable to properly quantify this yearly cycle. Once more data becomes available, we can (more appropriately) treat this yearly variability as a second seasonal term, D_t^*, and leave T_t to account for variability spanning multiple years.

A.1.1   Isolation of Trend Component

We use LOWESS, a non-parametric local regression technique, to isolate the monthly trend in VOC data. This method combines multiple linear regression and k-nearest-neighbors to produce a smooth curve. We provide more details of this fitting procedure below.

Consider the data (x_i, y_i) and assume the relationship

$$y_i = g(x_i) + \epsilon_i,$$

where g is a smooth function and the ϵ_i are random variables with mean zero and constant variance. LOWESS creates an estimate, $\hat{y}_i$, for each $g(x_i)$.

Each $\hat{y}_i$ is based on a neighborhood of x_i, such that only x_j in the neighborhood of x_i are used to estimate $\hat{y}_i$. Let $f \in (0, 1]$ be the proportion of x_j that influence $\hat{y}_i$. Therefore, f controls the size of the neighborhood around x_i. Larger values of f result in a smoother collection of $\hat{y}_i$, and vice versa. When estimating the long-term trend in VOC concentrations, we use cross-validation to select the optimal value of f. Furthermore, x_j in the neighborhood of x_i are given more weight if they are closer to x_i. Let $W(x)$ be a weight function that determines the relative influence of x_j in determining $\hat{y}_i$. This weight function must meet a number of conditions specified in [31]. A typical choice (and what was used to detrend the Canary VOC data) is the tri-cube weight function given by

$$w(x) = (1 - |d|^3)^3,$$

where d is the distance between x_i and x_j scaled to be on the range [0,1]. This weight function is applied to all x_j in the neighborhood of x_i.

Given f and W, each $\hat{y}_i$ is produced by weighted multiple linear regression using x_j in the neighborhood defined by f. An nth order polynomial is fit to these x_j, where n is typically small (i.e. $n = 1$ or $n = 2$). We implement this method using the `lowess` function from the *stats* package in R (available on CRAN). The `lowess` function also uses an iterative method to create "robustness weights" that insulate the estimates $\hat{y}_i$ from outliers. We will not discuss these additional weights here, but the interested reader can see [31] for reference.

To summarize, we estimate the trend component of the VOC signal by applying the LOWESS smoother described here to the entire time span of the VOC data. We create a separate estimate for each Canary unit.

A.1.2 Isolation of Seasonal Component

Recall that we are using the seasonal component, D_t, to capture diurnal variability in the VOC signal. Namely, we are interested in a smooth curve that represents the "average" or "typical" variation in VOCs over the course of the day. We go a step further by creating separate estimates for each month. This allows us to check one of the assumptions of the additive decomposition model described above (that the magnitude of the variability captured by D_t is independent of time t).

Before creating our estimates, we first subtract our estimated T_t from the VOC signal. This leaves us with only D_t plus R_t (assuming that we have created a good estimate of T_t), which is centered around zero. We then separate these detrended data by Canary unit and by month, since we want a separate D_t estimate for each.

Having prepared the data, we can estimate D_t. We begin by binning the detrended VOC data by minute and taking the median of each bin. We use the median instead of the mean to better insulate our estimate from large outliers in the signal (some of which are highlighted earlier in this document). Plotting these medians over time gives a noisy estimate of the diurnal cycle for a given unit and month. We finally apply a LOWESS smoother to the noisy estimate to create the curves shown in Figure 5.

Note that Figure 5 does not present confidence intervals of any kind. This was done for visual clarity. The method for estimating D_t described here does allow for some measure of uncertainty, however. It would be straightforward to construct a percentile interval based on the sampling distribution of the median for each bin using a technique called bootstrapping.

A.1.3 Isolation of Residual Component

With estimates for both T_t and D_t in hand, estimating the residual component R_t is fairly straightforward. We subtract our estimate for both T_t and D_t from the original VOC signal y_t. This leaves us with the residual component. As discussed in Section 4.1, it is advantageous to use this residual component (as opposed to the original signal y_t) when training predictive models. Doing this enables the models to better detect the anomalous events of interest represented by the residual component (i.e. a VOC leak event), rather than the naturally occurring trends in the data.

References

[1] "Columbia | SIPA Center on Global Energy Policy | Nowhere to Hide: Implications for Policy, Industry, and Finance of Satellite-Based Methane Detection," https://www.energypolicy.columbia.edu/research/commentary/nowhere-hide-implications-policy-industry-and-finance-satellite-based-methane-detection, October 2020, (Accessed on 12/09/2020).

[2] Environmental Protection Agency, "Oil and natural gas sector: Emission standards for new, reconstructed, and modified sources," *40 CFR 60, 81 FR 35823*, 2016.

[3] A. P. Ravikumar and A. R. Brandt, "Designing better methane mitigation policies: the challenge of distributed small sources in the natural gas sector," *Environmental Research Letters*, vol. 12, no. 4, p. 044023, apr 2017. [Online]. Available: https://doi.org/10.1088/1748-9326/aa6791

[4] "Environmental Defense Fund | The climate impacts of methane emissions," https://www.edf.org/climate-impacts-methane-emissions, April 2012, (Accessed on 12/09/2020).

[5] C. Davis, "Natural Gas Intelligence | Natural Gas Suppliers Urge Cutting Methane Emissions to Maintain Social License to Operate," https://www.naturalgasintel.com/natural-gas-suppliers-urge-cutting-methane-emissions-to-maintain-social-license-to-operate/, October 2020, (Accessed on 12/09/2020).

[6] "The colorado case study on methane emissions: Conversations with the oil and gas industry," 2016, https://keatingresearch.com/wp-content/uploads/2016/04/Colorado-Methane-Regulation-7-Survey-Research-Memo-4-10-2016-Final-Version.pdf.

[7] "Crestone peak resources announces new partnership for real-time well site air quality monitoring," 2020, https://www.projectcanary.com/crestone-peak-resources-announces-new-partnership-for-real-time-well-site-air-quality-monitoring/.

[8] "Stellae Energy | Energy Transition #6: How the Upstream Industry Can Reduce GHG Emissions," http://stellaeenergy.com/energy-transition-6-how-the-upstream-industry-can-reduce-ghg-emissions, August 2020, (Accessed on 12/09/2020).

[9] H. Hu, J. Landgraf, R. Detmers, T. Borsdorff, J. Aan de Brugh, I. Aben, A. Butz, and O. Hasekamp, "Toward global mapping of methane with tropomi: First results and intersatellite comparison to gosat," *Geophysical Research Letters*, vol. 45, no. 8, pp. 3682–3689, 2018. [Online]. Available: https://agupubs.onlinelibrary.wiley.com/doi/abs/10.1002/2018GL077259

[10] C. Frankenberg, I. Aben, P. Bergamaschi, E. J. Dlugokencky, R. van Hees, S. Houweling, P. van der Meer, R. Snel, and P. Tol, "Global column-averaged methane mixing ratios from 2003 to 2009 as derived from sciamachy: Trends and variability," *Journal of Geophysical Research: Atmospheres*, vol. 116, no. D4, 2011. [Online]. Available: https://agupubs.onlinelibrary.wiley.com/doi/abs/10.1029/2010JD014849

[11] A. Butz, S. Guerlet, O. Hasekamp, D. Schepers, A. Galli, I. Aben, C. Frankenberg, J.-M. Hartmann, H. Tran, A. Kuze, G. Keppel-Aleks, G. Toon, D. Wunch, P. Wennberg, N. Deutscher, D. Griffith, R. Macatangay, J. Messerschmidt, J. Notholt, and T. Warneke, "Toward accurate co2 and ch4 observations from gosat," *Geophysical Research Letters*, vol. 38, no. 14, 2011. [Online]. Available: https://agupubs.onlinelibrary.wiley.com/doi/abs/10.1029/2011GL047888

[12] S.-M. Li, A. Leithead, S. G. Moussa, J. Liggio, M. D. Moran, D. Wang, K. Hayden, A. Darlington, M. Gordon, R. Staebler, P. A. Makar, C. A. Stroud, R. McLaren, P. S. K. Liu, J. O'Brien, R. L. Mittermeier, J. Zhang, G. Marson, S. G. Cober, M. Wolde, and J. J. B. Wentzell, "Differences between measured and reported volatile organic compound emissions from oil sands facilities in alberta, canada," *Proceedings of the National Academy of Sciences*, vol. 114, no. 19, pp. E3756–E3765, 2017. [Online]. Available: https://www.pnas.org/content/114/19/E3756

[13] M. R. Johnson, D. R. Tyner, S. Conley, S. Schwietzke, and D. Zavala-Araiza, "Comparisons of airborne measurements and inventory estimates of methane emissions in the alberta upstream oil and gas sector," *Environmental Science & Technology*, vol. 51, no. 21, pp. 13 008–13 017, 2017, pMID: 29039181. [Online]. Available: https://doi.org/10.1021/acs.est.7b03525

[14] J. Peischl, T. B. Ryerson, K. C. Aikin, J. A. de Gouw, J. B. Gilman, J. S. Holloway, B. M. Lerner, R. Nadkarni, J. A. Neuman, J. B. Nowak, M. Trainer, C. Warneke, and D. D. Parrish, "Quantifying atmospheric methane emissions from the haynesville, fayetteville, and northeastern marcellus shale gas production regions," *Journal of Geophysical Research: Atmospheres*, vol. 120, no. 5, pp. 2119–2139, 2015. [Online]. Available: https://agupubs.onlinelibrary.wiley.com/doi/abs/10.1002/2014JD022697

[15] J. Peischl, A. Karion, C. Sweeney, E. A. Kort, M. L. Smith, A. R. Brandt, T. Yeskoo, K. C. Aikin, S. A. Conley, A. Gvakharia, M. Trainer, S. Wolter, and T. B. Ryerson, "Quantifying atmospheric methane emissions from oil and natural gas production in the bakken shale region of north dakota," *Journal of Geophysical Research: Atmospheres*, vol. 121, no. 10, pp. 6101–6111, 2016. [Online]. Available: https://agupubs.onlinelibrary.wiley.com/doi/abs/10.1002/2015JD024631

[16] J. G. Englander, A. R. Brandt, S. Conley, D. R. Lyon, and R. B. Jackson, "Aerial interyear comparison and quantification of methane emissions persistence in the bakken formation of north dakota, usa," *Environmental Science & Technology*, vol. 52, no. 15, pp. 8947–8953, 2018, pMID: 29989804. [Online]. Available: https://doi.org/10.1021/acs.est.8b01665

[17] G. Pétron, A. Karion, C. Sweeney, B. R. Miller, S. A. Montzka, G. J. Frost, M. Trainer, P. Tans, A. Andrews, J. Kofler, D. Helmig, D. Guenther, E. Dlugokencky, P. Lang, T. Newberger, S. Wolter, B. Hall, P. Novelli, A. Brewer, S. Conley, M. Hardesty, R. Banta, A. White, D. Noone, D. Wolfe, and R. Schnell, "A new look at methane and nonmethane hydrocarbon emissions from oil and natural gas operations in the colorado denver-julesburg basin," *Journal of Geophysical Research: Atmospheres*, vol. 119, no. 11, pp. 6836–6852, 2014. [Online]. Available: https://agupubs.onlinelibrary.wiley.com/doi/abs/10.1002/2013JD021272

[18] A. Karion, C. Sweeney, E. A. Kort, P. B. Shepson, A. Brewer, M. Cambaliza, S. A. Conley, K. Davis, A. Deng, M. Hardesty, S. C. Herndon, T. Lauvaux, T. Lavoie, D. Lyon, T. Newberger, G. Pétron, C. Rella, M. Smith, S. Wolter, T. I. Yacovitch, and P. Tans, "Aircraft-based estimate of total methane emissions from the barnett shale region," *Environmental Science & Technology*, vol. 49, no. 13, pp. 8124–8131, 2015, pMID: 26148550. [Online]. Available: https://doi.org/10.1021/acs.est.5b00217

[19] S. Schwietzke, M. Harrison, T. Lauderdale, K. Branson, S. Conley, F. C. George, D. Jordan, G. R. Jersey, C. Zhang, H. L. Mairs, G. Pétron, and R. C. Schnell, "Aerially guided leak detection and repair: A pilot field study for evaluating the potential of methane emission detection and cost-effectiveness," *Journal of the Air & Waste Management Association*, vol. 69, no. 1, pp. 71–88, 2019, pMID: 30204538. [Online]. Available: https://doi.org/10.1080/10962247.2018.1515123

[20] A. P. Ravikumar, S. Sreedhara, J. Wang, J. Englander, D. Roda-Stuart, C. Bell, D. Zimmerle, D. Lyon, I. Mogstad, B. Ratner *et al.*, "Single-blind inter-comparison of methane detection technologies–results from the stanford/edf mobile monitoring challenge," *Elementa: Science of the Anthropocene*, vol. 7, 2019.

[21] M. Omara, M. R. Sullivan, X. Li, R. Subramanian, A. L. Robinson, and A. A. Presto, "Methane emissions from conventional and unconventional natural gas production sites in the marcellus shale basin," *Environmental Science & Technology*, vol. 50, no. 4, pp. 2099–2107, 2016, pMID: 26824407. [Online]. Available: https://doi.org/10.1021/acs.est.5b05503

[22] D. T. Allen, V. M. Torres, J. Thomas, D. W. Sullivan, M. Harrison, A. Hendler, S. C. Herndon, C. E. Kolb, M. P. Fraser, A. D. Hill, B. K. Lamb, J. Miskimins, R. F. Sawyer, and J. H. Seinfeld, "Measurements of methane emissions at natural gas production sites in the united states," *Proceedings of the National Academy of Sciences*, vol. 110, no. 44, pp. 17 768–17 773, 2013. [Online]. Available: https://www.pnas.org/content/110/44/17768

[23] B. Franco, E. Mahieu, L. K. Emmons, Z. A. Tzompa-Sosa, E. V. Fischer, K. Sudo, B. Bovy, S. Conway, D. Griffin, J. W. Hannigan, K. Strong, and K. A. Walker, "Evaluating ethane and methane emissions associated with the development of oil and natural gas extraction in north america," *Environmental Research Letters*, vol. 11, no. 4, p. 044010, apr 2016. [Online]. Available: https://doi.org/10.1088/1748-9326/11/4/044010

[24] E. Atherton, D. Risk, C. Fougère, M. Lavoie, A. Marshall, J. Werring, J. P. Williams, and C. Minions, "Mobile measurement of methane emissions from natural gas developments in northeastern british columbia, canada," *Atmospheric Chemistry and Physics*, vol. 17, no. 20, pp. 12 405–12 420, 2017. [Online]. Available: https://acp.copernicus.org/articles/17/12405/2017/

[25] G. Pétron, G. Frost, B. R. Miller, A. I. Hirsch, S. A. Montzka, A. Karion, M. Trainer, C. Sweeney, A. E. Andrews, L. Miller, J. Kofler, A. Bar-Ilan, E. J. Dlugokencky, L. Patrick, C. T. Moore Jr., T. B. Ryerson, C. Siso, W. Kolodzey, P. M. Lang, T. Conway, P. Novelli, K. Masarie, B. Hall, D. Guenther, D. Kitzis, J. Miller, D. Welsh, D. Wolfe, W. Neff, and P. Tans, "Hydrocarbon emissions characterization in the colorado front range: A pilot study," *Journal of Geophysical Research: Atmospheres*, vol. 117, no. D4, 2012. [Online]. Available: https://agupubs.onlinelibrary.wiley.com/doi/abs/10.1029/2011JD016360

[26] A. P. Ravikumar, J. Wang, and A. R. Brandt, "Are optical gas imaging technologies effective for methane leak detection?" *Environmental Science & Technology*, vol. 51, no. 1, pp. 718–724, 2017, pMID: 27936621. [Online]. Available: https://doi.org/10.1021/acs.est.6b03906

[27] R. Subramanian, L. L. Williams, T. L. Vaughn, D. Zimmerle, J. R. Roscioli, S. C. Herndon, T. I. Yacovitch, C. Floerchinger, D. S. Tkacik, A. L. Mitchell, M. R. Sullivan, T. R. Dallmann, and A. L. Robinson, "Methane emissions from natural gas compressor stations in the transmission and storage sector: Measurements and comparisons with the epa greenhouse gas reporting program protocol," *Environmental Science & Technology*, vol. 49, no. 5, pp. 3252–3261, 2015, pMID: 25668051. [Online]. Available: https://doi.org/10.1021/es5060258

[28] A. P. Ravikumar, D. Roda-Stuart, R. Liu, A. Bradley, J. Bergerson, Y. Nie, S. Zhang, X. Bi, and A. R. Brandt, "Repeated leak detection and repair surveys reduce methane emissions over scale of years," *Environmental Research Letters*, vol. 15, no. 3, p. 034029, feb 2020. [Online]. Available: https://doi.org/10.1088/1748-9326/ab6ae1

[29] J. Fialka, "Scientific American | Meet the Satellites That Can Pinpoint Methane and Carbon Dioxide Leaks," https://www.scientificamerican.com/article/meet-the-satellites-that-can-pinpoint-methane-and-carbon-dioxide-leaks/, March 2018, (Accessed on 12/09/2020).

[30] "Project Canary | Canary Air Quality Monitoring," https://www.projectcanary.com/collect, (Accessed on 12/09/2020).

[31] W. S. Cleveland, "Robust locally weighted regression and smoothing scatterplots," *Journal of the American Statistical Association*, vol. 74, no. 368, pp. 829–836, 1979. [Online]. Available: http://www.jstor.org/stable/2286407